DOI: 10.1002/ejoc.200800429

A Full Conformational Characterization of Natural Ionones and Irones, as well as 13-Alkyl-Substituted α-Ionones

Laura Legnani,[a] Marco Luparia,[a] Giuseppe Zanoni,[a] Lucio Toma,*[a] and Giovanni Vidari[a]

Keywords: Molecular modeling / Density functional calculations / Fragrances / Terpenoids / Olfactory properties

A modeling study at the B3LYP/6–31G(d) level was performed on a group of natural odorants. These included α-, β-, and γ-ionones, β-irone, *cis*- and *trans*-α- and -γ-irones, and three synthetic α-ionone analogues, all containing an identical *E*-enone moiety and differing in the *endo* or *exo* positions of another double bond and an additional alkyl group at C(2) or at C(13). Data showed a shift of the conformational preference of the butenone chain from an axial or pseudoaxial orientation, as favored in α-ionone and in *trans*-α- and -γ-irones, to an equatorial or pseudoequatorial orientation, as favored in γ-ionone and in *cis*-α- and -γ-irones. These changes have been correlated with the enhanced olfactory potencies of the latter set of compounds. In the synthetic α-ionone analogues, bearing an ethyl, propyl, or isobutyl group at C(5) instead of the methyl group present in α-ionone, the hindrance due to this alkyl group does not affect the overall conformational behavior of the molecules. The odor properties seem to be modulated by specific hydrophobic interactions of each carbon of this C(5) alkyl chain with some olfactory receptors rather than by different distributions of the conformational populations.

Introduction

With the increasing launch rates of perfumes, there is an increasing demand for new odorants. A slight structural modification of a known odorant can meet this need because it often results in a significant change in the olfactory properties. However, the de novo *rational* design of more efficient odorants based on the concept of molecular complementarity to a receptor surface is still considered to be virtually hopeless, contrarily to the case of most drug–receptor interactions.[1] In fact, the human olfactory system, being made up of about 350 G protein-coupled receptors,[2] uses combinatorial coding schemes to encode odor entities.[3] The total pattern of receptor signaling reaching the higher brain is eventually interpreted in terms of odor notes and facets, threshold, and/or perceived intensity. With an array of many different receptors stimulated by odorant molecules, the construction of a static olfactophore model (a special case of a pharmacophore model) – that is, a representation of generalized molecular features that are responsible for a given odor – is therefore considered to have limited value for the prediction of all the subtle odorant characteristics. Consequently, the design of a new odorant relies heavily on structural similarities to a reference compound.[4] In this context, knowledge of the 3D geometries of odorants with well established odor properties can provide some insight into the molecular features associated with a given odor, at least with regard to the predominant note(s) at the threshold level, at which only the receptor(s) of highest affinity are presumably stimulated.[5] Such structure–odor relationships can be more firmly established by examination of the structural features of components of the same family, in which the contributions of different electronic, stereoelectronic, steric, and conformational properties of strictly related molecules can be more easily compared and distinguished.[6] Moreover, knowledge of the conformational space of structurally related odorants is a requisite for studies of the interactions of these compounds with an olfactory receptor model. Indeed, although no quaternary structure of a human olfactory receptor site is known so far, modeling on the crystal structure of bovine rhodopsin, which has a high homology to certain human receptors, has in some cases allowed quite accurate prediction of the odor threshold.[5]

Many odorants share pleasant woody-floral, violet ionone-like scent characteristics. They include well known natural fragrance components, such as α-, β-, and γ-ionones (**1**–**3**), irones **4**–**8**, and different synthetic derivatives such as, among others, dihydro and tetrahydro analogues,[7,8] bicyclo[6.4.0]dodecene ketone **9**,[9] the seven-membered ring compound **10**,[10] the octahydrodecaline Georgywood® (**11**),[4b] and *seco*-ionones Koavone® (**12**)[4b] and **13**.[11] Such a large variety of different structures clearly makes it diffi-

[a] Dipartimento di Chimica Organica, Università di Pavia, Via Taramelli 10, 27100 Pavia, Italy
Fax: +39-0382-987323
E-mail: lucio.toma@unipv.it

Supporting information for this article is available on the WWW under http://www.eurjoc.org or from the author.

cult to define an "ionone olfactophore", based on molecular parameters common to the entire group, even if the excellent superposition of the 3D skeletons of compound **9** and β-ionone **2**,[4b] as well of **12** and 10-methylionone,[12] provided explanations for their similar odor profiles. Anyhow, these findings clearly indicate the need to refine the early assertion by Jitkow and Bogert[13] relating to the critical dependence of the ionone violet odor on the presence of a cyclohexene nucleus carrying at least three methyl groups, two of them adjacent to the 3-oxobut-1-enyl chain.

In this paper we have limited our modeling study, at the B3LYP/6–31G(d) level, to a restricted group of woody floral odorants: namely ionones **1**–**3**, irones **4**–**8**, and synthetic ionone derivatives **14**–**16**, all containing the same (*E*)-but-2-enone moiety but differing in the position of another double bond and an additional alkyl group at C(2) or at C(13). Modeling of more diversified structures, such as **9**–**13**, will be considered in further studies.

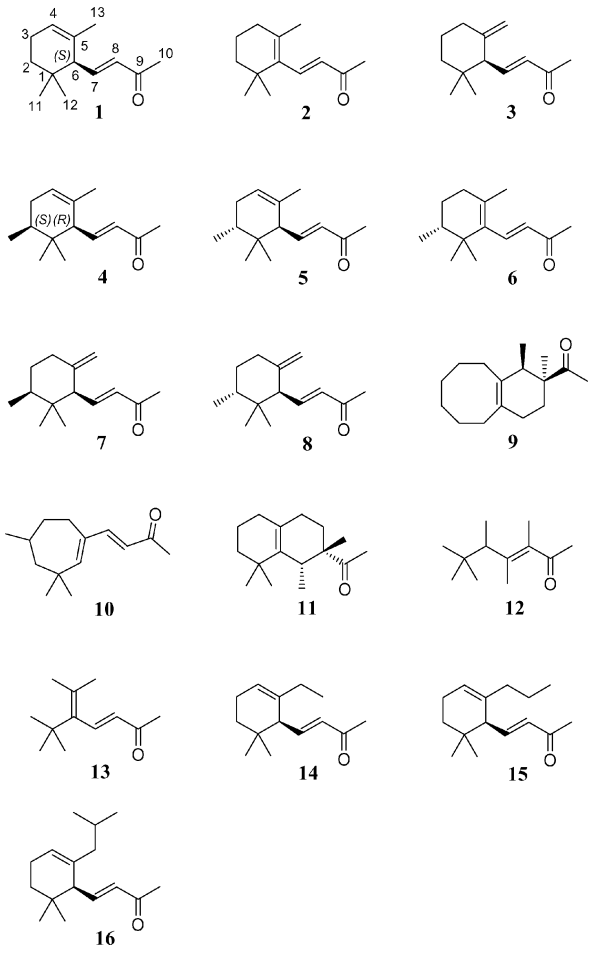

Regioisomeric ionones **1**–**3**, occurring in the headspace of different flowers in bloom, constitute one of the most important group of perfumery raw materials,[14] and are of great economic value in the creation of violet and many other odor notes. Moreover, they are used as starting materials in several industrial processes, and have also served as valuable building blocks in the synthesis of different other natural products.[15] Irones, isolated from the rhizomes of different *Iris* species,[8] can be considered the most pleasant and precious naturally occurring 2-alkyl-substituted ionones used in the perfume industry. Synthetic 13-alkyl-substituted ionones **14** and **16** first appeared in patents some time ago[16] and, along with **15**, have recently been synthesized by us in enantiomerically pure forms as a part of a program directed towards the synthesis of ionone analogues and their olfactory evaluation.[17]

The relationship between molecular structure and odor characteristics in this group has not yet been examined systematically, although scattered studies on the preferred conformations of α-ionone (**1**),[18a,18c] and *cis*- (**4**) and *trans*-α-irone[18a,18b] (**5**) have appeared in the literature. Recently, the dramatic dependence of olfactory properties of ionones and irones on their chiralities has been clearly demonstrated.[8] Therefore, in this paper we have assumed the absolute configuration at C(6) of compounds **1**, **3**–**5**, **7**, **8**, and **14**–**16** to be the same as in (*S*)-α-ionone (**1**), which corresponds to the more powerful antipode both in the ionone and in the irone series.[8] Odor properties discussed in this paper are, therefore, of these stereoisomers.

Results and Discussion

The conformational space of compounds **1**–**8** and **14**–**16** was explored by optimization of all the possible starting geometries by the DFT approach at the B3LYP level with the 6–31G(d) basis set.[19] All the degrees of conformational freedom were considered, in particular the possible existence of different chair or half-chair conformations of the hexacyclic ring, as well as the orientation of the butenone chain at C(6) and the alkyl substituent at C(5).

Several conformations were located for each compound; Table 1, Table 2, Table 3, and Table 4 summarize the main geometrical data, together with the relative energy of each conformation and its percentage contribution to the overall population determined through the Boltzmann equation. The geometry of the ring is described through two descriptors: a significant torsion angle – τ_R [C(3)–C(2)–C(1)–C(6)] – and the ring puckering coordinates determined as described by Cremer and Pople.[20] The orientation of the butenone chain is described through the torsion angles τ_1 [C(1)–C(6)–C(7)–C(8)] and τ_2 [C(7)–C(8)–C(9)–C(10)], whereas the orientation of the alkyl group at C(5) in compounds **14**–**16** is described through appropriate torsion angles. The most representative conformations of each compound are shown as three-dimensional plots in Figures 1, 2, and 4–7.

Eight conformations of α-ionone (**1**) were located (Table 1); the global minimum **1A**, which accounts for more than 50% of the overall population, shows a $^2HC_1$ half-chair geometry (see the ring puckering coordinates in Table 1), a pseudoaxial orientation of the butenone chain, and a *cisoid* arrangement of the α,β-unsaturated ketone (Figure 1). In **1A**, the plane of the unsaturated ketone is almost perpendicular to the mean plane of the hexacyclic ring, with an angle ω of 96° between the two planes. Con-

Table 1. Geometrical features, relative energies, and equilibrium percentages of the conformations of ionones **1**–**3** (the bold characters highlight the data for the global minimum conformations).

	E_{rel} [kcal mol^{-1}]	%	τ_R [°][a]	τ_1 [°][b]	τ_2 [°][c]	ω [°]	Ring puckering coordinates		
							Q	ϕ_2	θ
1A	**0.00**	**51.5**	**59**	**124**	**179**	**96**	**0.48**	**–161**	**132**
1B	0.68	16.4	58	124	0	95	0.47	–162	132
1C	0.73	15.1	60	–105	180	83	0.49	–162	131
1D	1.61	3.4	60	–104	1	83	0.49	–162	131
1E	0.94	10.5	–61	109	180	76	0.49	29	50
1F	1.68	3.0	–61	110	0	76	0.49	30	50
1G	3.70	0.1	–61	–96	–179	57	0.50	35	51
1H	4.56	0.0	–61	–94	1	59	0.50	32	50
2A	**0.00**	**18.2**	**42**	**137**	**178**	**140**	**0.49**	**–95**	**127**
2B	0.95	3.7	43	134	0	138	0.49	–86	127
2C	0.06	16.6	46	–137	–178	48	0.47	–93	132
2D	1.12	2.7	46	–135	1	50	0.47	–93	132
2I	0.47	8.2	44	10	–179	16	0.50	–88	126
2J	1.97	0.6	45	12	1	18	0.50	–90	126
2E	0.06	16.6	–46	137	178	132	0.47	93	48
2F	1.12	2.7	–46	135	–1	130	0.47	93	48
2G	**0.00**	**18.2**	**–42**	**–137**	**–178**	**40**	**0.49**	**95**	**53**
2H	0.95	3.7	–43	–134	0	42	0.49	86	53
2 K	0.47	8.2	–44	–10	179	164	0.50	88	54
2 L	1.97	0.6	–45	–12	–1	162	0.50	90	54
3A	0.18	32.8	54	122	–179	88	0.54	–141	178
3B	1.13	6.6	54	120	–1	87	0.54	–139	178
3C	1.37	4.4	55	–143	178	75	0.55	–158	177
3D	2.39	0.8	56	–141	0	75	0.55	–155	177
3E	**0.00**	**44.5**	**–56**	**119**	**–179**	**92**	**0.56**	**–4**	**3**
3F	0.84	10.8	–56	119	0	90	0.56	–1	3
3G	3.70	0.1	–56	–75	180	80	0.56	–3	3
3H	4.55	0.0	–56	–74	1	82	0.56	–1	3

[a] τ_R: C3–C2–C1–C6. [b] τ_1: C1–C6–C7–C8. [c] τ_2: C7–C8–C9–C10.

Table 2. Relative energies and equilibrium percentages of the conformations of irones **4**–**8** (the bold characters highlight the data for the global minimum conformations).

	E_{rel} [kcal mol^{-1}]	%		E_{rel} [kcal mol^{-1}]	%
4A	1.65	4.5	**7A**	2.81	0.7
4B	2.34	1.4	**7B**	3.73	0.1
4C	3.04	0.4	**7C**	2.89	0.6
4D	4.00	0.1	**7D**	4.02	0.1
4E	**0.00**	**72.7**	**7E**	**0.00**	**80.1**
4F	0.76	20.3	**7F**	0.88	18.2
4G	2.93	0.5	**7G**	3.71	0.2
4H	3.79	0.1	**7H**	4.55	0.0
5A	**0.00**	**56.7**	**8A**	**0.00**	**63.0**
5B	0.67	18.2	**8B**	0.95	12.6
5C	0.68	17.9	**8C**	0.85	14.9
5D	1.56	4.1	**8D**	1.92	2.5
5E	1.87	2.4	**8E**	1.43	5.6
5F	2.61	0.7	**8F**	2.25	1.4
5G	4.49	0.0	**8G**	5.19	0.0
5H	5.39	0.0	**8H**	6.07	0.0
6A	**0.00**	**31.2**	**6E**	0.83	7.7
6B	0.94	6.3	**6F**	1.88	1.3
6C	0.04	29.0	**6G**	0.82	7.7
6D	1.10	4.8	**6H**	1.76	1.6
6I	0.80	8.0	**6 K**	1.76	1.6
6J	2.33	0.6	**6 L**	3.19	0.1

Table 3. Relative energies and equilibrium percentages of the conformations of compound **14**.

	E_{rel} [kcal mol^{-1}]	%	Σ%[a]	τ_3 [°][b]
14Aa	0.00	26.7		76
14Ab	1.24	3.3	51.0	–99
14Ac	0.14	21.0		–177
14Ba	0.63	9.2		77
14Bb	1.96	1.0	16.9	–98
14Bc	0.82	6.7		–176
14Ca	0.71	8.0		77
14Cb	2.12	0.7	14.6	–63
14*Cc*	0.89	5.9		–177
14Da	1.62	1.7		77
14Db	3.02	0.2	3.4	–62
14Dc	1.72	1.5		–176
14Ea	0.84	6.4		66
14Eb	1.92	1.0	10.9	–92
14Ec	1.21	3.5		173
14Fa	1.56	1.9		66
14Fb	2.80	0.2	3.1	–96
14Fc	1.98	1.0		174
14Ga	3.61	0.1	0.1	59
14Gc	4.25	0.0		168
14Ha	4.52	0.0	0.0	58
14Hc	5.09	0.0		168

[a] Σ%: overall percentage contribution of each family. [b] τ_3: C6–C5–C13–C14.

Table 4. Relative energies and equilibrium percentages of the selected conformations of compounds **15**–**16**.

	E_{rel} [kcal mol^{-1}]	%	Σ%[a]	τ_3 [°][b]
15Aa	0.00	29.4	50.7	78
15Ba	0.61	10.5	16.9	77
15Ca	0.70	9.1	14.7	80
15Da	1.63	1.9	3.2	78
15Ea	0.85	7.0	11.2	67
15Fa	1.57	2.1	3.2	67
15Ga	3.58	0.1	0.1	59
15Ha	4.52	0.0	0.0	59
16Aa	0.00	32.5	52.3	76
16Ba	0.66	10.7	15.5	76
16Ca	0.70	10.0	13.5	76
16Da	1.65	2.0	2.8	76
16Ea	0.74	9.4	12.3	67
16Fa	1.46	2.8	3.6	102
16Ga	3.56	0.1	0.1	59
16Ha	4.46	0.0	0.0	58

[a] Σ%: overall percentage contribution of each family. [b] τ_3: C6–C5–C13–C14.

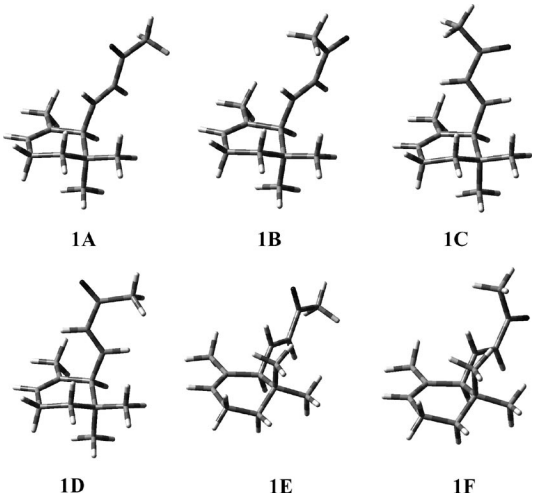

Figure 1. 3D plot of the most representative conformations of α-ionone (**1**).

formers **1B**–**D**, all showing the same pseudoaxial orientation of the butenone moiety, present similar values of this angle (ω = 83–95°). The four conformers differ instead in the orientation of the butenone substituent: the preferred ones (**1A** and **1B**) are characterized by an *anti* arrangement of 6-H and 7-H ($\tau_1 \approx 120°$), whereas the other two (**1C** and **1D**) show a *syn* arrangement ($\tau_1 \approx -100°$). The α,β-unsaturated ketone unit prefers the *cisoid* arrangement ($\tau_2 \approx 180°$, **1A** and **1C**) over the *transoid* one ($\tau_2 \approx 0°$, **1B** and **1D**). The remaining populated conformations **1E**–**H**, which account for an overall percentage of 13.6%, arise from ring inversion to the $^1HC_2$ half-chair geometry. In these conformations the butenone moiety is pseudoequatorial, the angle ω is smaller (57–76°) than in **1A**–**D**, whereas τ_1 and τ_2 maintain the same preference as shown in **1A**–**D**. The *anti* arrangement of 6-H and 7-H, observed in **1A**, **1B**, **1E**, and **1F**, is thus favored for 81.4% of cases and the *cisoid* arrangement of the α,β-unsaturated ketone, observed in **1A**, **1C**, **1E**, and **1G**, accounts for 77.2%. Our calculations thus confirm the preference of the side chain for a pseudoaxial orientation, also deduced from the CD spectrum of compound **1**,[18b] as well as the *anti* arrangement of 6-H and 7-H, supported by the value of the corresponding observed ^{1}H NMR coupling constant.[18c] Both the *cisoid* and *transoid* arrangements of the α,β-unsaturated ketone are predicted to be populated by our calculations (77% and 23%, respectively), in agreement with the enhancement of both the 7-H and 8-H NMR signals upon irradiation of the acetyl methyl group of **1**[18c] and with a NOESY experiment (see Supporting Information) performed by us on a commercial sample of **1**. Notably, the B3LYP/6–31G(d) modeling predicted a higher stability for the *cisoid* arrangement, contrary to empirical calculations, which predicted a preference for the *transoid* one.[18c]

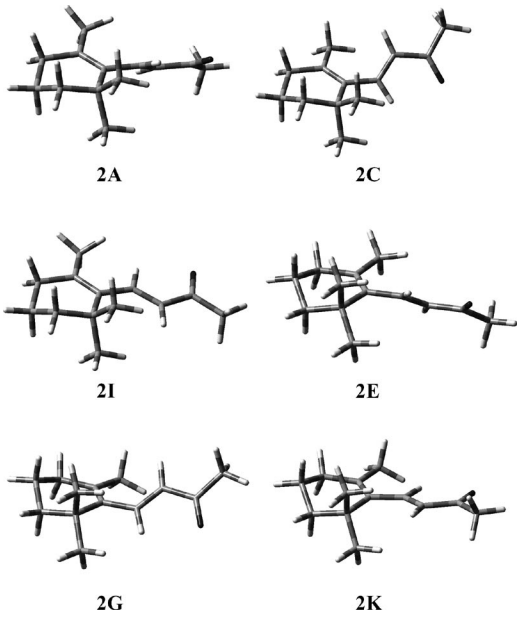

Figure 2. 3D plot of the most representative conformations of β-ionone (**2**).

The different location of the double bond in β-ionone **2**, in relation to the α-isomer **1**, affects its conformational behavior significantly. In fact, in **2** the butenone chain is linked to a planar trigonal carbon atom instead of a tetrahedral stereogenic carbon atom, and conjugation of the carbonyl group extends further to the γ and δ positions represented by the C(6) and C(5) carbon atoms, respectively. These structural elements force the butenone chain of **2** to protrude from the hexacyclic ring with an orientation resembling the equatorial arrangement assumed in conformations **1E**–**G** (Figure 2). Moreover, in spite of the extended conjugation, the plane of the unsaturated ketone and the mean plane of the hexacyclic ring are not coplanar, because of the steric interactions of the three methyl groups at C(5) and C(1) with the butenone chain, so the ω angle is significantly different from 0° or 180°, assuming values indicating a deviation from coplanarity of as much as 50° (Table 1). Moreover, the cyclohexene ring in **2** assumes, as in **1**, only

half-chair geometries: namely the $^2HC_3$ and $^3HC_2$ conformations. The $^2HC_3$ conformations are reported in Table 1 as **2A**–**D** and **2I**–**J**, while the $^3HC_2$ conformations, which are enantiomeric to them, are reported as **2E**–**H** and **2K**–**L**. Superimposition of conformations **2A** and **2E** with **1A** and **1E**, respectively, obtained through root mean square fitting of the atoms of the ring (Figure 3), shows the close resemblance of the **E** geometries, contrarily to the **A** geometries, where the orientations of the butenone chains are quite different.

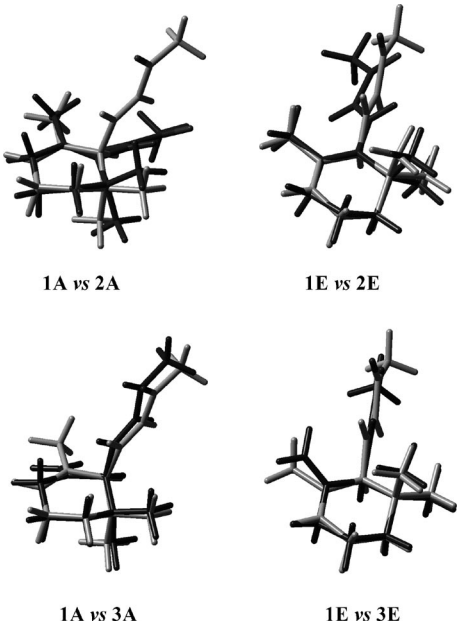

Figure 3. Overlaps of conformations **A** and **E** of α-ionone (**1**, gray shading) and β-ionone or γ-ionone (**2** or **3**, respectively, black shading), obtained through rms fitting of the atoms of the ring.

γ-Ionone (**3**) showed conformational behavior similar to that of its regioisomer **1**; however, appreciable differences were observed. As in the case of **1**, eight conformations were located (Table 1, Figure 4) and each of them resembled the corresponding conformation of **1**; see, for example, the overlaps of **3A** to **1A** and of **3E** to **1E** (Figure 3). However, the energy ranking changed quite considerably, with the global minimum energy conformation **3E** showing a chair geometry occupying the opposite region of the conformational space with respect to **1A** (θ = 3° in **3E**, in comparison with θ = 132° in **1A**). Actually, conformations **3E**–**H**, characterized by this inverted chair conformation, account for 55.4% of the overall population, thus making the equatorial orientation of the butenone moiety preferred over the axial one. The other conformational preferences of the butenone unit of γ-ionone (**3**) were maintained as in the α-isomer **1**: a 94.7% preference for the *anti* arrangement of 6-H and 7-H and an 81.8% preference of the unsaturated ketone system for the *cisoid* arrangement. As in **1**, the angle ω assumes values close to 90°, in particular in the most populated conformations.

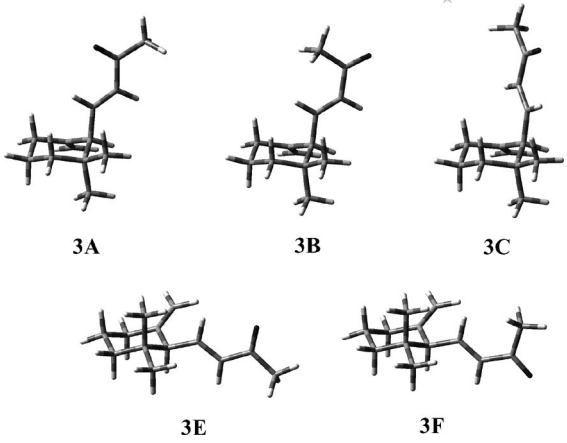

Figure 4. 3D plot of the most representative conformations of γ-ionone (**3**).

Ionones (*S*)-**1**, **2**, and (*S*)-**3** each possess a pleasant floral-woody odor with a pronounced violet tonality; however, **2** and **3** are about 20 and 40 times more powerful than **1**, respectively.[8] The increased potency of **2** and **3** relative to **1** would thus seem to be linked to a shift in the conformational equilibrium towards geometries leading to a pseudo-equatorial orientation of the butenone chain.

Relative to ionones **1**–**3**, α-, β-, and γ-irones each present an additional methyl group, which creates a stereogenic center, at C(2). In α- and γ-irones this methyl group may be oriented *cis* or *trans* to the butenone chain, giving rise to the two pairs of diastereoisomers: **4**/**5** and **7**/**8**, respectively. Notably, odor potency and tonalities vary within the group and with respect to **1** and **3**.[8] The odor of the two *cis*-irones **4** and **7** thus shows a warm floral-woody tonality; in addition, the smell of the α-isomer **4** has a distinct "orris butter" character, while that of the γ-isomer **7** possesses some fruity nuances and green aspects. Interestingly, **7** and the β-irone enantiomer **6** show a similar β-ionone-type odor.[8] In contrast, *trans*-α-irone (**5**) shows a weak violet-woody character devoid of the characteristic soft "orris" tone, whereas the odor of *trans*-γ-irone (**8**) has only a weak woody tonality.[8] Moreover, *cis* isomers are considerably more potent than the corresponding *trans* isomers. It is thus clear that the increased steric hindrance near C(2), due to the methyl substituent, could not account entirely for such odor differences with respect to ionones. Actually, molecular modeling shows different molecular topologies for the structures **4**, **5**, **7**, and **8** (Figure 5). As is the case of **1**, a group of eight different conformations could be located for each of the compounds **4**, **5**, **7**, and **8**; however, the energy rankings of the conformations relative to **1** were different, in a way that could easily be interpreted. As expected, conformations in which the C(2) methyl group is pseudoaxially oriented – namely the $^2HC_1$ conformations of **4** and the $^1HC_2$ conformations of **5** – are destabilized, so in **4** the $^2HC_1$ conformations **4A**–**D** became much less favored (6.4%) than the $^1HC_2$ conformations **4E**–**H** (93.6%), whereas in the case of **5** the preference for the $^2HC_1$ geometry was further enhanced (**5A**–**D**, 96.9%). The other confor-

mational preferences for the α-irones **4** and **5** remained almost the same as in α-ionone (**1**): the *anti* 6-H/7-H preference was 98.9 and 78.0%, respectively, whereas the *cisoid* arrangement of the α,β-unsaturated ketone was 78.1 and 77.0%, respectively.

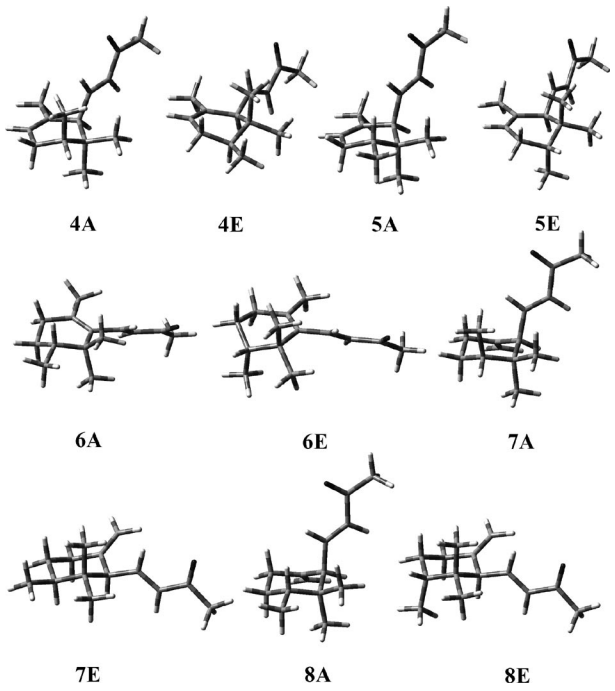

Figure 5. 3D plot of the most representative conformations of irones **4**–**8**.

In the case of γ-irones **7** and **8**, the C(2) methyl group exerts the same effects as shown for the α-isomers **4** and **5**, respectively, destabilizing the conformations in which it is axially oriented (Figure 5). The *cis* isomer **7** largely prefers the chair conformations **7E**–**H** (98.4%), in which both the substituents at C(2) and C(6) are equatorially oriented. On the other hand, the *trans* isomer **8** prefers the opposite chair conformations **8A**–**D** (93.0%) in which the methyl group at C(2) is equatorial and the butenone chain is forced into an axial orientation. The usual conformational preferences were also maintained for compounds **7** and **8**: the *anti* 6-H/7-H preferences were 99.1 and 82.6%, respectively, whereas the *cisoid* arrangements of the α,β-unsaturated ketone were 81.6 and 83.5%, respectively. In conclusion, within the two pairs of α- and γ-irones (**4**, **5** and **7**, **8**, respectively) the better olfactory properties are shown in each case by the diastereoisomer presenting a greater preference of the butenone chain for the pseudoequatorial or equatorial orientation: namely by the *cis* stereoisomers **4** and **7**. Moreover, odor potency increases for irones (**4**, **7** vs. **5**, **8**) with the C(1)–βCH_3 axially oriented in the most populated conformations (**4E**, **7E** vs. **5A**, **8A**), in a fashion similar to that seen with γ-ionone (**3**) relative to α-ionone (**1**). On the other hand, hardly identifiable is a single structural factor clearly related to the lack of the "orris-butter" tonality among the characters of *trans*-α-irone (**5**). Presumably, this characteristic note is linked to a cooperative effect of various structural motifs.

With respect to the conformational behavior, β-irone **6** showed a great similarity to β-ionone (**2**), nicely paralleling the odor properties.[8] However, the presence of the stereocenter at C(2) and the consequent equatorial or axial orientations assumable by the C(2) methyl groups, differentiate, on energetic grounds, the **A**–**D/I**–**J**, and the **E**–**H/K**–**L** groups of conformations, though they maintain the same geometry of the ring and of the butenone chain as assumed in the corresponding conformation of **2**. As would be expected, the latter group of conformations are destabilized, although, with the exception of **6L**, their percentage contributions are not negligible.

The three synthetic compounds **14**–**16**,[17] which can be considered α-ionone homologues with increased steric hindrance around C(13), were then modeled. Eight conformations, as found for **1**, were located for **14**; however, the substitution of the olefinic methyl with an ethyl group introduces an additional degree of freedom, giving rise to three possible orientations, described by the torsion angle τ_3 [C(6)–C(5)–C(13)–C14]. The eight geometries, labeled as **A**–**H**, thus give rise in the case of **14** to conformational families, each containing three members. In Table 3 every individual conformation is described and the overall percentage contribution of each family is also reported. The family percentages of compound **14** closely parallel the corresponding individual percentages of the conformations of compound **1**. This clearly indicates that substitution of the methyl group at C(5) by an ethyl moiety does not influence the overall conformational behavior of the molecule to any extent, so the $^2HC_1$ conformations **14A**–**D** are preferred as in the natural compound **1**. The $^1HC_2$ half-chair conformations **14E**–**H** account for a percentage of 14.1%. The ethyl group prefers the g^+ *gauche* and the *trans* orientations, whereas the g^- *gauche* orientation is less stable by more than 1 kcal mol^{-1}. Figure 6 shows 3D plots of the three members of the **14A** family, together with the members of the **14E** family.

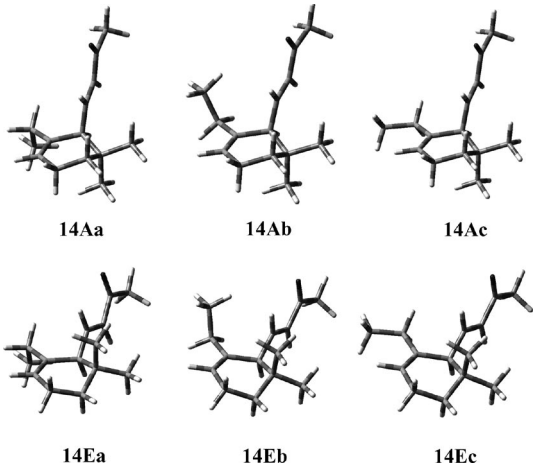

Figure 6. 3D plot of the three members of the **A** and **E** families of compound **14**.

The ionone analogues **15** and **16** were modeled identically to **14**. For these compounds, possessing bulkier groups at C(5) than **14**, the members of every families in-

creased numerically because of the higher number of degrees of freedom associated with the alkyl groups. However, only the most populated member of each family is reported in Table 4; its individual percentage contribution to the overall population is accompanied by the value corresponding to the entire family. Once again, the family percentage values proved to be very similar to those of **1**. Figure 7 shows the most populated $^2HC_1$ and $^1HC_2$ conformations of **15** and **16**.

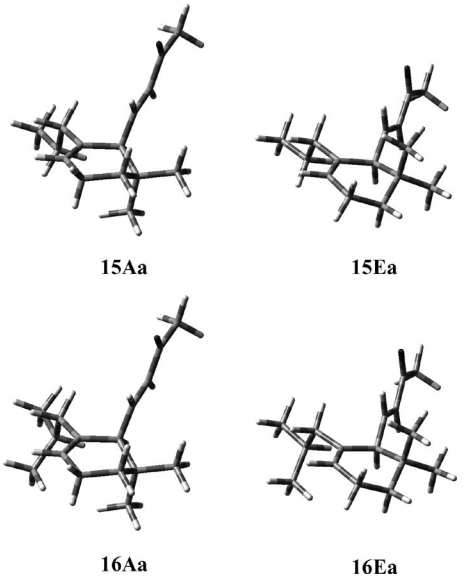

Figure 7. 3D plot of the most populated $^2HC_1$ and $^1HC_2$ conformations of compounds **15** and **16**.

Olfactory evaluation of compounds **14**–**16** (*Givaudan Schweiz AG, Fragrance Research*) showed that enhanced steric hindrance around the cyclohexene double bond does not significantly affect the predominant ionone-like tonalities of the series, while it introduces additional distinct notes, such as the orris facets displayed by the propyl derivative **15**.[17] The 5-ethyl ionone homologue **14** was the most powerful of the three compounds on blotter; indeed, its odor threshold – 0.085 ng per L of air[17] – was more than thirty times lower than the parent α-ionone (**1**, 2.7 ng per L of air), and of the same order of magnitude as γ-ionone (**3**, 0.07 ng per L of air), which is regarded as the most powerful and pleasant isomer.[8] In contrast, the isobutyl derivative **16** was the weakest odorant of these three synthetic ionones on blotter.[17] The progressive decrease in the potency of **15** and **16** in relation to **14** indicates that the potential for accommodation of a group larger than methyl is limited to the size of an ethyl group. Groups as large as propyl or isobutyl hinder positive interaction with some olfactory receptors (ORs). The better olfactory properties of compound **14** in relation to **1** seem to be due to specific interactions of C(14) rather than to a different distribution of the conformational population. The preference for the *trans* and the g^+ orientations suggests one of these two orientations as responsible for the activity of compound **14**. Conformationally constrained analogues, in which the ethyl group is frozen in a precise orientation, could allow the active orientation to be established and might even lead to more potent odorants. Apparently, specific hydrophobic interactions of each carbon of the C(5)-alkyl chain with ORs modulate the individual additional notes accompanying the predominant ionone-like odors of compounds **1** and **14**–**16**.

Conclusions

In this paper we have described a complete B3LYP/6–31G(d) modeling study of α-, β-, and γ-ionones and irones **1**–**8** and their synthetic analogues **14**–**16**, each containing an identical *E*-enone moiety, and differing in the *endo* or *exo* position of the other double bond and the additional presence of an alkyl group at C(2) or at C(13).

The modeling study showed a shift of the conformational preferences of the butenone chain from a pseudoaxial orientation, favored in **1**, to a pseudoequatorial one, favored in **2** and **3**, suggesting this steric factor to be related to the increased olfactory potency of **2** and **3** in relation to **1**. Analogously, the better odor properties of the *cis*-irones **4** and **7** in relation to the *trans* stereoisomers **5** and **8** seem to be linked to a greater preference of the butenone chain for assuming a pseudoequatorial or an equatorial orientation.

In contrast, the hindrance of the alkyl group at C(5) does not significantly affect the overall conformational behavior of synthetic α-ionone analogues **14**–**16**; however, it seems to be the main factor affecting the odor potency of these compounds. Moreover, conformational analysis of compound **14** suggests that rigid analogues, in which the two-carbon moiety at C(5), being incorporated in a cyclic structure, would be frozen in a precise orientation, could enable us to establish the active orientation and might even lead to more potent odorants. This stimulates the design of new derivatives of ionones **1** and **14**, the syntheses of which will be pursued in our laboratories. Their preparations and the determined odor properties, in relation to those of parent compounds **1** and **14**, should be reported in the near future.

Computational Methods

All the calculations were carried out by use of the GAUSSIAN03 program package.[21] The conformational space of compounds **1**–**8**, **14**–**16** was explored through optimization of all the possible starting geometries, which were optimized by the DFT approach at the B3LYP level with the 6–31G(d) basis set. All the degrees of conformational freedom were considered. Vibrational frequencies were computed at the same level of theory to verify that the optimized structures were minima.

Supporting Information (see footnote on the first page of this article): Torsion angles τ_R, τ_1, and τ_2, ω angle, and ring puckering coordinates of compounds **4**–**8**, **14**–**16**; energies in Hartrees and Cartesian coordinates of all reported conformations of compounds **1**–**8**, **14**–**16**; NOESY spectrum of compound **1**.

Acknowledgments

This work was supported by the Italian Ministero dell'Università e della Ricerca (MIUR) (COFIN grants) and by the University of

Pavia (FAR grants). We thank CILEA for the allocation of computer time.

[1] C. S. Sell, *Angew. Chem. Int. Ed.* **2006**, *45*, 6254–6261.
[2] a) L. Buck, R. Axel, *Cell* **1991**, *65*, 175–187; b) R. Axel, *Angew. Chem. Int. Ed.* **2005**, *44*, 6111–6127; c) L. B. Buck, *Angew. Chem. Int. Ed.* **2005**, *44*, 6128–6140; d) S. Zozulya, F. Echeverri, T. Nguyen, *Adv. Genome Biol.* **2001**, *2*, research 0018.1–0018.12.
[3] B. Malnic, J. Hirono, T. Sato, L. B. Buck, *Cell* **1999**, *96*, 713–723.
[4] a) G. Fráter, J. A. Bajgrowicz, P. Kraft, *Tetrahedron* **1998**, *54*, 7633–7703; b) P. Kraft, J. A. Bajgrowicz, C. Denis, G. Fráter, *Angew. Chem. Int. Ed.* **2000**, *39*, 2980–3010; c) *The Chemistry of Fragrances* (Ed.: C. Sell), The Royal Society of Chemistry, Cambridge, United Kingdom, **2006**.
[5] L. Doszczak, P. Kraft, H.-P. Weber, R. Bertermann, A. Triller, H. Hatt, R. Tacke, *Angew. Chem. Int. Ed.* **2007**, *46*, 3367–3371.
[6] As one referee has underlined, other factors such as ligand volatility, solubility, and lipophilicity, as well as intrinsic entropic factors, are also important in determining the olfactory properties of compounds[4c].
[7] C. Chapuis, R. Brauchli, *Helv. Chim. Acta* **1993**, *76*, 2070–2088.
[8] E. Brenna, C. Fuganti, S. Serra, *Tetrahedron: Asymmetry* **2003**, *14*, 1–42.
[9] P. Kraft, *Synthesis* **1999**, 695–703.
[10] M. Stoll, W. Scherrer, *Helv. Chim. Acta* **1940**, *23*, 941–948.
[11] K. Sestanj, *Croat. Chem. Acta* **1962**, *34*, 211–217.
[12] C. B. Warren, W. E. Brugger, G. S. Zander, *Chem. Ind. London* **1983**, *1*, 36–38.
[13] O. N. Jitkow, M. T. Bogert, *J. Am. Chem. Soc.* **1941**, *63*, 1979–1984.
[14] K. Bauer, D. Garbe, H. Surburg, *Common Fragrance and Flavor Materials*, 4th ed., Wiley-VCH, Weinheim, Germany, **2001**.
[15] E. Brenna, C. Fuganti, S. Serra, P. Kraft, *Eur. J. Org. Chem.* **2002**, 967–978 and references cited therein.
[16] a) W. C. Meuly, P. S. Gradeff, to *Rhodia Inc.*, U. S. Pat. 3,480,677 (*Chem. Abstr.* **1970**, *72*, 21805t); b) R. Kaiser, to *Givaudan Corporation*, Eur. Pat. EP 3515 (*Chem. Abstr.* **1979**, *92*, 42165).
[17] M. Luparia, P. Boschetti, F. Piccinini, A. Porta, G. Zanoni, G. Vidari, *Chem. Biodiv.* **2008**, *5*, 1045–1057.
[18] a) W. E. Steinmetz, *J. Am. Chem. Soc.* **1974**, *96*, 685–692; b) V. Rautenstrauch, B. Willhalm, W. Thommen, G. Ohloff, *Helv. Chim. Acta* **1984**, *67*, 325–331; c) N. Qing, L. D. Colebrook, F. Commodari, *Magn. Reson. Chem.* **1991**, *29*, 459–464.
[19] a) A. D. Becke, *J. Chem. Phys.* **1993**, *98*, 5648–5652; b) C. Lee, W. Yang, R. G. Parr, *Phys. Rev. B* **1988**, *37*, 785–789.
[20] D. Cremer, J. A. Pople, *J. Am. Chem. Soc.* **1975**, *97*, 1354–1358.
[21] M. J. Frisch, G. W. Trucks, H. B. Schlegel, G. E. Scuseria, M. A. Robb, J. R. Cheeseman, J. A. Montgomery Jr., T. Vreven, K. N. Kudin, J. C. Burant, J. M. Millam, S. S. Iyengar, J. Tomasi, V. Barone, B. Mennucci, M. Cossi, G. Scalmani, N. Rega, G. A. Petersson, H. Nakatsuji, M. Hada, M. Ehara, K. Toyota, R. Fukuda, J. Hasegawa, M. Ishida, T. Nakajima, Y. Honda, O. Kitao, H. Nakai, M. Klene, X. Li, J. E. Knox, H. P. Hratchian, J. B. Cross, C. Adamo, J. Jaramillo, R. Gomperts, R. E. Stratmann, O. Yazyev, A. J. Austin, R. Cammi, C. Pomelli, J. W. Ochterski, P. Y. Ayala, K. Morokuma, G. A. Voth, P. Salvador, J. J. Dannenberg, V. G. Zakrzewski, S. Dapprich, A. D. Daniels, M. C. Strain, O. Farkas, D. K. Malick, A. D. Rabuck, K. Raghavachari, J. B. Foresman, J. V. Ortiz, Q. Cui, A. G. Baboul, S. Clifford, J. Cioslowski, B. B. Stefanov, G. Liu, A. Liashenko, P. Piskorz, I. Komaromi, R. L. Martin, D. J. Fox, T. Keith, M. A. Al-Laham, C. Y. Peng, A. Nanayakkara, M. Challacombe, P. M. W. Gill, B. Johnson, W. Chen, M. W. Wong, C. Gonzalez, J. A. Pople, *Gaussian 03*, Revision B.04, Gaussian, Inc., Pittsburgh PA, **2003**.

Received: April 30, 2008
Published Online: August 20, 2008

